Response of copepods to physical gradients associated with structure in the ocean

C. B. Woodson[1] *and D. R. Webster*
School of Civil and Environmental Engineering, Georgia Institute of Technology, Atlanta, Georgia 30332

M. J. Weissburg and J. Yen
School of Biology, Georgia Institute of Technology, Atlanta, Georgia 30332

Abstract

We studied the response of the copepods *Acartia tonsa* and *Temora longicornis* to spatial gradients of flow velocity and fluid density to determine whether the presence of physical gradients initiated local search for resources or promoted aggregation. Two additional species of copepods, *Candacia ethiopica* and *Labidocera madurae,* were also exposed to velocity gradients. A plane jet flume apparatus facilitated the isolation of physical structures that mimic those found in the ocean and permitted high-resolution behavioral observations. All four species significantly increased the proportion of time in the gradient layer region relative to the total time in the observation window (proportional residence time) in response to the velocity-gradient layer. Behavioral changes, such as increased swimming speed and turn frequency, were consistent with area-restricted search behavior. *T. longicornis* also significantly increased proportional residence time in response to the density-gradient layer, but changes in swimming speed and turn frequency were not significantly different. *A. tonsa* and *T. longicornis* appeared to contact the density gradient and swim away or along the boundary. Hence, density gradients may act as a barrier to vertical movement and not as a positive cue for area-restricted search behavior. Velocity and density gradients play important, yet different, roles in defining patterns at fine-to-intermediate scales in zooplankton ecology.

Historically, ecological patterns in the plankton have been attributed to large-scale physical forcing; however, recent studies and observations have led to a realization that behavioral interactions of organisms to physical or chemical features at fine-to-intermediate scales may also be important (Franks 1995; Yamazaki et al. 2002; Gallager et al. 2004). Additionally, the ability of copepods to locate patches of high productivity is directly linked to survival (Mullin and Brooks 1976; Daro 1988); hence, behavioral responses of organisms at these scales will influence population dynamics and community structure (Alldredge et al. 2002; Cowles 2004). Ephemeral food patches in the ocean are often associated with steep gradients in physical properties, and behavioral adaptations that limit search to these regions may be advantageous (Poulet and Ouellet 1982; Buskey 1984; Daro 1988; Tiselius 1992; Saiz et al. 1993; Bochdansky and Bollens 2004).

Many observations suggest that a large proportion (>75%) of phytoplankton biomass in a water column can be concentrated into one or a few well-defined regions (Holliday et al. 2003). These patches, often termed thin layers, may be 10s of centimeters thick, possibly less (Cowles et al. 1998), and are commonly associated with boundaries separating different bodies of water (Dekshenieks et al. 2001). Zooplankton, such as copepods, are known to aggregate at these boundaries (Holliday et al. 1998), but basic questions regarding copepod foraging behavior and sensory response to oceanic structure remain unanswered. Association between physical gradients and food presence provides a cue that foraging copepods can utilize to focus searches near regions likely to have high concentrations of resources. Once the copepod is in the proximity of a physical gradient, the scales of interactions may be appropriate for chemical sensing or direct contact with food particles. Can copepods utilize environmental gradients (physical and chemical) associated with thin layers to narrow searches for food, mates, or other resources? If so, which physical features do copepods utilize to cue area-restricted search behavior, thus improving foraging efficiency? Copepods should display behavioral changes in response to physical gradients if individuals use these gradients as cues to direct search patterns.

Hydrodynamic disturbances, such as velocity gradients, are sensed by copepods via the differential bending of finely-tuned mechanoreceptive setae on their antennae (Fields et al. 2002). Copepods use fluid disturbances as predator avoidance cues (Strickler 1977; Yen and Fields 1992; Titelman 2001) and for mate and prey capture (Strickler 1998; Yen et al. 1998). Copepods escape most consistently in response to the shear strain rate of the surrounding flow, with threshold levels varying among copepod species and stages from 0.4–26 s^{-1} (Yen and Fields 1992; Fields and Yen 1997*a,b*; Kiørboe et al. 1999; Titelman 2001; Titelman and Kiørboe 2003*a,b*). These behavioral thresholds are well above physiological-detection thresholds reported by Fields et al. (2002) for *Gaussia princeps,* and the magnitude of physiological limits are believed to be of the same order of magnitude for other species.

Changes in density can provide cues or act as barriers to migrating zooplankton that lead to aggregation at these boundaries (Harder 1968; Tiselius et al. 1994; Lougee et al. 2002). Harder (1968) observed that *T. longicornis* aggregated to a density gradient in the absence of a salinity gradient but did not aggregate to a salinity gradient without a density change, which suggests that the response is likely to be mechanically and not chemically mediated. Density gradients can alter sinking and/or swimming speed and consequently change the velocity of the animal relative to the surrounding fluid. Thus, organisms may sense density gradients in a similar fashion as a hydrodynamic disturbance or velocity gradient. Harder (1968) and Lougee et al. (2002) suggest that aggregation at these boundaries may be due to energetic advantages while suspended in the water column. More dense fluid requires less effort to maintain vertical position; however, a lighter fluid requires less inertial input to swim. Bochdansky and Bollens (2004) and others suggest that density gradients may also act as a positive cue for limiting search behavior. On the other hand, density differences may simply act as a physical or behavioral barrier to vertical migration (Harder 1968; Hamner 1988; Leising 2001). The mechanisms and motivations of copepod aggregation at physical discontinuities remain unresolved.

Several studies have assessed the importance of food presence and chemical stimulants in copepod foraging and swarming behavior (Poulet and Marsot 1978). Poulet and Ouellet (1982) showed that *Eurytemora hermanii* and *Acartia tonsa* swarm in response to dissolved amino acids associated with phytoplankton exudates at concentrations similar to observed field conditions. This swarming is analogous to an excited area-restricted search behavior in which animals increase swimming speed and turn more frequently to remain in the region of interest (Mauchline 1998). In the presence of actual food particles, Tiselius (1992) reports a reduction in swimming speed, which is likely associated with feeding bouts.

The conflicting results of these studies prevent a thorough evaluation of the impacts of patchiness and physical variability of the water column on zooplankton ecology. Is it possible that copepods can utilize gradients in velocity and/or density to recognize structure in the water column, thus cueing area-restricted search behavior? Reported in situ values of strain rate and density steps in the thin-layers literature (e.g., Dekshenieks et al. 2001) are lower than escape-response thresholds (e.g., Fields and Yen 1997a) but well above physiological limits (Fields et al. 2002). The influence of physical gradients on individual copepod behavior has not been previously examined and, until recently, resolution of in situ measurements was not sufficient to define appropriate field conditions for simulation in the laboratory (Cowles 2004). The studies discussed above have assessed the importance of density gradients on copepod aggregation and the use of velocity gradients in predator avoidance and mate capture. But none has used an individual-based approach to examine whether and how copepods utilize physical structure in pelagic habitats to improve foraging efficiency. In this study, we begin to assess the behavioral responses of individual copepods to physical gradients in the water column and how these responses compare with known behav-
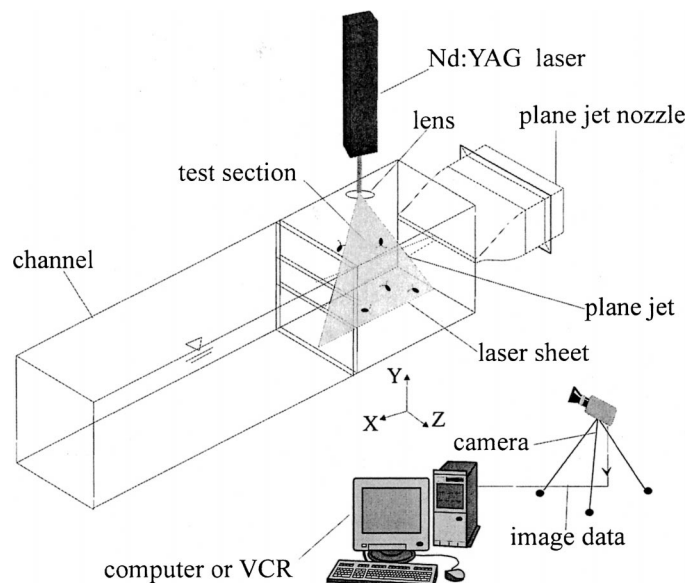

Fig. 1. Sketch of the experimental apparatus for physical measurements (PIV/LIF). For behavioral observations, the Nd:YAG laser is replaced with a 14-Watt 640-nm illumination unit or infrared diodes.

iors that may lead to aggregation, such as area-restricted search behavior.

Methods

A model thin layer generated in the lab enabled observations of copepod behavioral responses to well-quantified, small-scale stimuli. Fluid velocity and density gradients characteristic of field conditions were established in a specially designed apparatus. A clear acrylic tank (100 cm × 30 cm × 30 cm) with a stainless-steel slot jet nozzle mounted on one end was used for both physical characterization and behavioral experiments (Fig. 1). The model layer generated in this apparatus consisted of either a velocity or density gradient in absence of food (phytoplankton) to insure that copepod responses are specific to these physical gradients. The nozzle exit was 1.0 cm tall and extended over the full interior width of the tank (25 cm). The operating water depth in the tank was 28 cm. The 10-cm × 10-cm test section corresponded to the region from 5 to 15 cm downstream of the nozzle exit. This configuration resulted in a velocity gradient layer that covered the middle third of the observation window. Observations were conducted in the transverse center of the tank to insure that the tank walls did not influence the flow and movement patterns of copepods.

Physical measurements—A constant-head tank supplied the plane jet flow of artificial seawater (Instant Ocean) for the velocity gradient layer experiments. The plane jet was uniform in the transverse, or *z*-direction (along the axis of the camera), eliminating the need for three-dimensional analysis. A top-hat velocity profile at the nozzle exit was insured by using a fifth-order polynomial to define the contraction shape (e.g., Hussein 1994). The flow passed through a sym-

metrical flow retrieval/conditioning structure at the end of the test section and then to an isolated reservoir tank. A remote pump (Dolphin Pumps, #DP-800) returned water to the constant-head tank mounted 1 m above the test tank. This arrangement minimized disturbances and provided a constant, steady flow to the plane jet nozzle.

A nonintrusive imaging technique, called particle image velocimetry (PIV), was employed (e.g., Raffel et al. 1998) to quantify the velocity gradient layer. This technique measured the displacement of small tracer particles ($\sim$5 μm, titanium dioxide spheres) over short time delays. A thin laser sheet, generated by an Nd:YAG laser (532-nm wavelength, New Wave Technologies Minilase III), and 1-m focal length spherical and -12.6-mm focal length cylindrical lenses illuminated the tracer particles in a vertical plane aligned with the flow direction (Fig. 1). A charged coupled device (CCD) camera (Redlake MegaPlusES 1.0 with a 105 mm Nikon Micro-Nikkor lens; $1,018\times1,008$ pixels) provided images with resolution of 0.1 mm per pixel. Images were recorded digitally at a rate of 10 Hz over a 25-s period. Sequential images were analyzed by subwindow (32×32 pixel) cross-correlation using a code developed by Dasi (2004). Dividing the displacement estimate for each subwindow by the time delay between the images yielded a sequence of instantaneous velocity fields. The fields were then filtered and ensemble averaged.

Density gradients were created at the interface between fluids with different salinity. Experiments were prepared by first filling the tank halfway with 30 salinity artificial seawater. Using a small pump (Dolphin Pumps #DP-400), a denser (32 salinity) volume of artificial seawater was slowly pumped into the tank through the drain fitting until the interface between the two fluids was located at the middle of the tank. Planar laser-induced fluorescence (PLIF) was used to quantify the density gradient created by the change in salinity. Minute quantities of fluorescent dye (50 μg l^{-1} Rhodamine 6G) were used as a tracer for salt concentration and the intensity of emitted light from the dye was linearly proportional to the concentration. The molecular diffusion coefficient of Rhodamine 6G ($\sim$10^{-9} m^2 s^{-1}) and salt ($\sim$10^{-9} m^2 s^{-1}) are essentially the same, making this a valid technique over the time scales of these experiments (Webster et al. 2003). A laser sheet (532 nm, same arrangement as described above for PIV) was used to excite the dye, causing it to fluoresce (peak emission around 565 nm). An optical cut-off filter (Tiffen color 21) blocked the green laser light and only allowed the fluoresced light to pass to the CCD camera (Redlake MegaPlus ES 1.0). Temperature variations that cause density gradients were not employed due to difficulty in establishing and maintaining consistency over the duration of the behavioral experiments.

Behavioral experiments and the flow field analysis were performed with a jet exit velocity, U_j, of 6.7 mm s^{-1}. The selected flow rate was the most stable of those tested, covered the range of reported in situ shear strain rate values, and did not yield strain rates above escape-response thresholds for documented species. The jet was laminar in the observation section for these target strain rates, which assured that the flow gradient was steady and repeatable. Therefore, organism reactions could be matched to the measured ve-

locity field based on their location in the field of view. Density gradients were established with a salinity change of 2 ($\Delta\sigma_t = 1.8$). This density change also corresponded well with reported field conditions and with gradients used in previous thin-layer–type experiments (Tiselius 1992; Bochdansky and Bollens 2004; Cowles 2004; Clay et al. 2004). Rhodamine 6G used for quantification of the density gradients was not present in the tank during behavioral experiments.

Behavioral observations and analysis—Copepods were collected at several locations and shipped overnight to Atlanta, Georgia, sorted by species, then transferred to holding tanks for a minimum of 2 d before experiments. Copepods were kept in culture in an environmental room that was adjusted to ambient water temperature based on location and season of the region where the animals were collected (12°C) or at the National Undersea Research Center in Key Largo, Florida. Four species of copepods, *Acartia tonsa, Temora longicornis, Labidocera madurae,* and *Candacia ethiopica,* were used in this study. *A. tonsa* were collected at the Skidaway Institute of Oceanography in Savannah, Georgia, and *T. longicornis* were collected from Stony Brook Harbor and from the Gulf of Maine. *C. ethiopica* and *L. madurae* were collected near Conch Reef in Key Largo, Florida.

Experiments were conducted in an environmental room at constant temperature (12 $\pm$ 0.2°C) and consisted of one of the following treatments: (1) a velocity gradient layer ($U_j = 6.7$ mm s^{-1}), (2) a density-gradient layer ($\Delta\sigma_t = 1.8$), or (3) a control with no gradient (stagnant tank). Each experiment was conducted in the same apparatus used for physical characterization (Fig. 1). with a slightly different observation arrangement. The Nd:YAG laser was replaced by a 14-W fluorescent lighting fixture fitted with a low-pass filter (Kodak Safelight #2A, 640 nm) or infrared diodes. Copepods did not respond to light at these wavelengths (Tiselius 1992; unpubl. data). A CCD video camera (Pulnix model TM-745, 768 $\times$ 494 pixels) with a 60-mm lens (Nikon Micro-Nikkor) was used for behavioral observations, and images were recorded via a video home system (VHS) video recorder.

Filtered artificial seawater (Instant Ocean) made from deionized water was used in all experiments in order to present animals only with the physical cues associated with each treatment. No food was present in the tank during experiments for the same reason. Species-specific groups of 60–70 mixed-sex copepods were added to the tank and aggregated at the surface or bottom using a fiber-optic light source until the start of experiments (approximately 10% remained at the surface or bottom during the experiment). The experiment began after a 2-h acclimation period. Animals were allowed to swim freely in the tank, and their positions in the 10-cm $\times$ 10-cm observation section were recorded for a period of 2 h. During an experiment, between 0 and 10 copepods were typically present in the observation window (mode around 2). A mesh filter (50 μm) was attached to the overflow at the end of the main tank to prevent copepods from traveling through the entire system and being visually sampled more than once.

Paths of swimming organisms were taken from VHS format and converted to data files containing coordinate posi-

tions using ExpertVision software (MotionAnalysis Corp.) at 15 Hz. This frame rate was selected because it provided sufficient displacement between frames to accurately assess swimming speed. The displacement of an animal swimming at 0.5 cm s^{-1} was roughly one pixel between consecutive frames for the image resolution of our system. Swimming speed calculations were not sensitive to the time interval of measurement for these settings. The digitized paths were filtered to remove paths with escape responses and paths that did not cross into the layer at least once during the time in the observation window. This resulted in a loss of between 0 and 10 paths for most species. For turn frequency and density-gradient crossing tests, the first 40 accepted paths were selected. A typical path lasted approximately 60 s for all experiments. Analysis of individual paths consisted of calculating proportional residence time, swimming speed, and turn frequency. The proportional residence time is the proportion of time in the layer relative to the total time in the viewing window. This eliminates bias associated with the Eulerian perspective because effects of shorter times in the viewing window resulting from flow advection are removed.

Swimming speed was defined as the speed relative to the flow velocity for copepods in the velocity gradient layer treatments and actual swimming speed for other treatments. Turn frequency was defined as the number of turn events per second, where a turn event was defined as a change in direction of motion of more than 15 degrees. Each of these kinematic parameters was computed for overall path, the portions of the path in versus out of the layer, and precontact versus postcontact with the physical gradient layer. Statistical comparisons of proportional residence time, swimming speed, and coefficient of variation were conducted using one-way analysis of variance (ANOVA) between control and treatments (proportional residence time) as well as precontact versus postcontact with the layer (path kinematics). Statistical evaluations of the coefficient of variation were also employed to evaluate changes in behavior.

Results

Physical measurements—Figure 2 shows the ensemble-averaged velocity field recorded during characterization experiments for a Reynolds number of 53 ($Re = U_jD/\nu$; $U_j = 6.7$ mm s^{-1}; $D = 10$ mm; $\nu = 1.27$ mm^2 s^{-1}). Plane jet flows for Reynolds numbers below 10 are laminar. Jets with Reynolds numbers around 50 are initially transitional but become laminar within a few nozzle widths of the jet exit. At higher Reynolds numbers, the jet becomes turbulent far downstream (Sato and Sakao 1964). The laminar regime for this flow was verified by minimal particle movement in the transverse direction and small values of the standard deviation of the velocity vectors. Maximum velocities in the observation section decreased from 6 mm s^{-1} at 5.0 cm downstream of the jet nozzle to 4 mm s^{-1} at 15.0 cm downstream. The corresponding velocity profile at $x = 10.5$ cm compared well with the analytical solution of Bickley (1937) for a plane jet (Fig. 3a). Local shear strain rates ($1/2[\partial u/\partial y + \partial v/\partial x]$) are shown as contours in Fig. 2. The other components of the
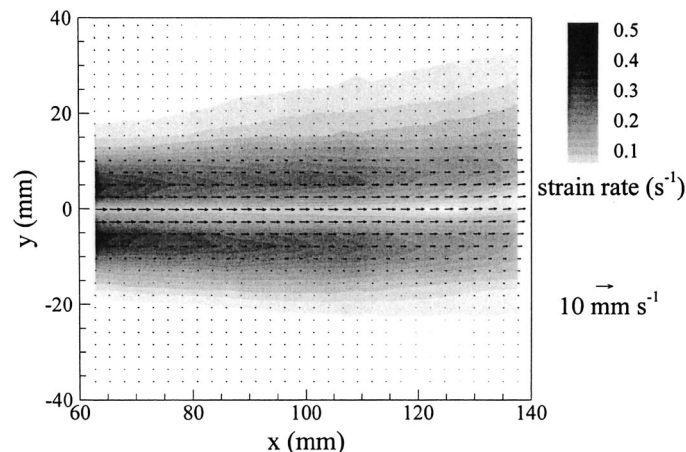

Fig. 2. Velocity and shear strain rate fields for $U_j = 6.7$ mm s^{-1}. Contours show the magnitude of the shear strain rate ($1/2[\partial u/\partial y + \partial v/\partial x]$) .

strain-rate tensor are an order of magnitude lower than the shear component and therefore are not shown here. The shear strain rate profiles also agreed well with the analytical solution of Bickley (1937; Fig. 3b). For the flow rate used here, maximum shear strain rates varied from 0.35 s^{-1} (at $x = 5$ cm) to 0.12 s^{-1} (at $x = 15$ cm) with distance downstream in the observation window. Across the layer, strain rates ranged from zero to the local maximum (0.12–0.35 s^{-1}) depending on location on the x-axis. For zooplankton behavior experiments, the boundary or edge of the layer, δ_S, was defined as the point where the shear-strain rate fell below 0.025 s^{-1}. Because copepods appeared to respond to strain rate, this definition of the boundary of the velocity gradient layer was more relevant for behavioral observations compared with the velocity half-width, δ, which is traditionally employed as a measure of velocity gradient layer thickness (Sato and Sakao 1964). Across the viewing window, the velocity layer grew linearly with distance downstream from a 17-mm half width (at $x = 5$ cm) to a 27-mm half width (at $x = 15$ cm) as defined by the strain rate threshold above.

While the range of shear strain rate in the apparatus covered the range reported in field estimates, the maximum values (0.12–0.35 s^{-1}) exceeded the maximum shear ($\partial u/\partial y$ only) recorded in situ for thin layers (0.1 s^{-1} reported by Dekshenieks et al. 2001). However, resolution restrictions of field velocity measurements (~20 cm at best; often closer to 1 m) suggest that strain rates estimated in the ocean may be much higher than reported. For example, Dekshenieks et al. (2001) utilized an acoustic Doppler current profiler (ADCP) with a minimum bin size of 1 m. For a strain rate equal to 0.05 s^{-1}, this corresponds to a change of 5 cm/s over the 1-m distance. The velocity change under density stratified conditions is likely to occur over a shorter distance, as evidenced by Cowles (2004). If the recorded change in velocity really occurred over a distance of 10 cm, then reported maximum strain rates would be equal to 0.5 s^{-1}. This is an extreme example, but it illustrates the need for higher resolution field measurements. It should be noted here that the oceanographic definition of shear ($\partial u/\partial y$) is related to,
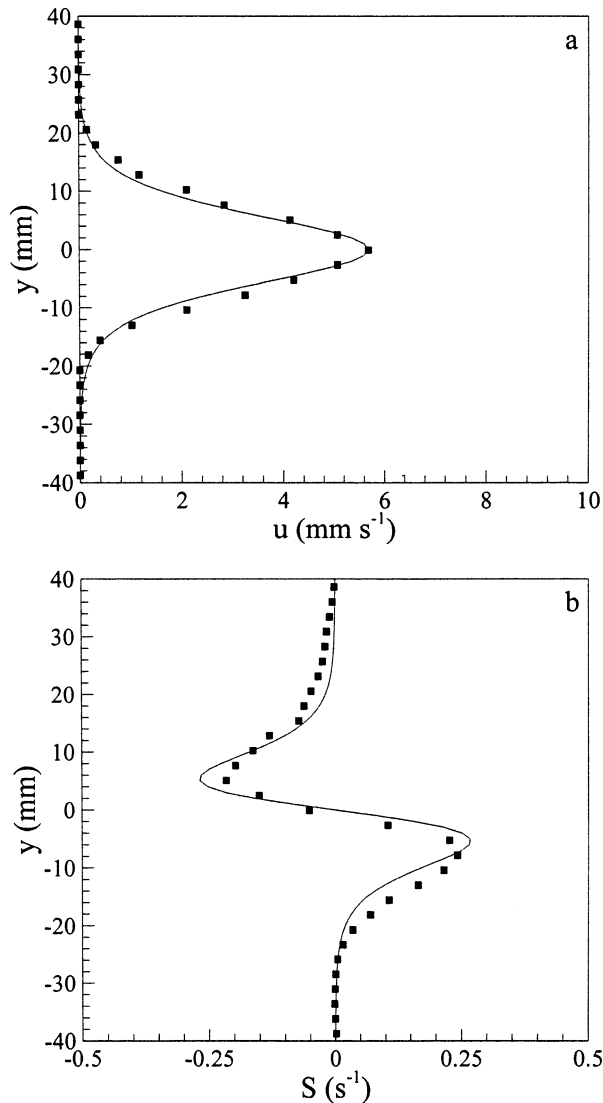
Fig. 3.   Comparison of the measured (a) velocity and (b) shear strain rate ($S = 1/2[\partial u/\partial y + \partial v/\partial x]$) profiles (shown with data points) at $x = 10.5$ cm to the analytical solution of Bickley (1937) indicated by a solid line.

Fig. 4.   Density profile at $x = 10.0$ cm. Salinity is 30 and 32 above and below the layer, respectively.

but distinctly different from, the fluid dynamic shear strain rate, $1/2(\partial u/\partial y + \partial v/\partial x)$, reported in this study. However, because the $(\partial u/\partial y)$-term dominated the shear strain rate, these values are similar (numerical values obviously differing by a factor of one half). Maximum shear strain rates in the model layer were always below reported escape response thresholds (Yen and Fields 1992; Fields and Yen 1997*a*; Titelman and Kiørboe 2003*a,b*).

Figure 4 shows an example density gradient 2 h after the tank is filled, corresponding to the beginning of the behavioral experiments. The salinity change of two between the upper and lower fluid layers resulted in a density discontinuity of approximately $1.8\sigma_t$ units. The upper and lower regions consisted of constant density similar to small-scale density steps reported by Cowles (2004), and the gradient is contained entirely within the vertical interval defined by the shear strain rate profiles. To alleviate effects of changes in
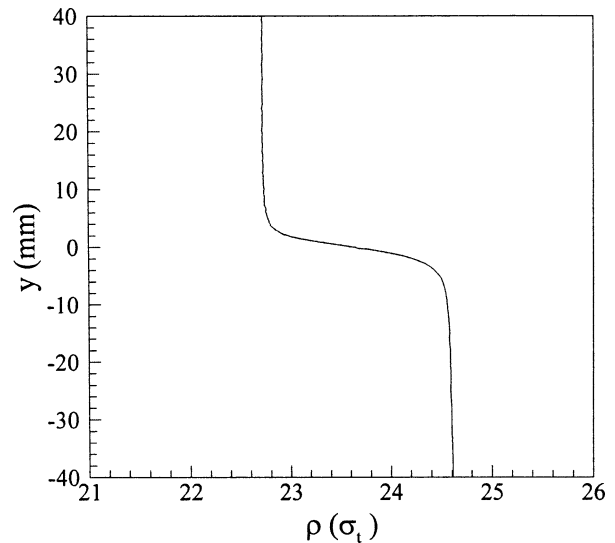
layer thickness, proportional residence time and other quantities are solely based on thickness of the layer defined by the velocity gradient treatment.

Behavioral experiments—Copepod species responded to both of the physical gradient layers, although in differing fashions. Most copepods showed attractive or excited behavior in the presence of the velocity gradient layer, but swam away from or along the density gradient. At the conclusion of the velocity gradient layer experiments, most, if not all, of the copepods were located in the rear channel section of the tank past the flow conditioner (Fig. 1), indicating that they were swept into this section by the flow during the experiment. Because copepods could swim against and out of the plane jet, this indicated a behavioral choice to remain within the layer. The accumulation of animals downstream of our visualization area also minimized the possibility of recording one animal multiple times during each experiment.

Proportional residence time in each gradient layer and for the control (no flow or density change) for all species tested is shown in Figs. 5 and 6. *T. longicornis* significantly increased proportional residence time in response to both velocity (degrees of freedom = 99, $F = 17.40$, $p < 0.001$) and density-gradient layers (degrees of freedom = 99, $F = 6.86$, $p < 0.001$), whereas *A. tonsa* exhibited significant increases in proportional residence time to the velocity gradient layer (degrees of freedom = 99, $F = 23.74$, $p < 0.001$) but not to the density-gradient layer (degrees of freedom = 99, $F = 0.50$, $p = 0.748$) compared to controls. *C. ethiopica* and *L. madurae* also significantly increased proportional residence time in the velocity gradient layer (degrees of freedom = 79, $F = 4.67$, $p = 0.017$, *C. ethiopica*; degrees of freedom = 59, $F = 22.01$, $p < 0.001$, *L. madurae*) versus controls (recall that these animals were not tested with density gradients). The low sample number for the *L. madurae* control (Tables 1 and 2) resulted from few paths being available over the course of the tape. Proportional residence times in con-
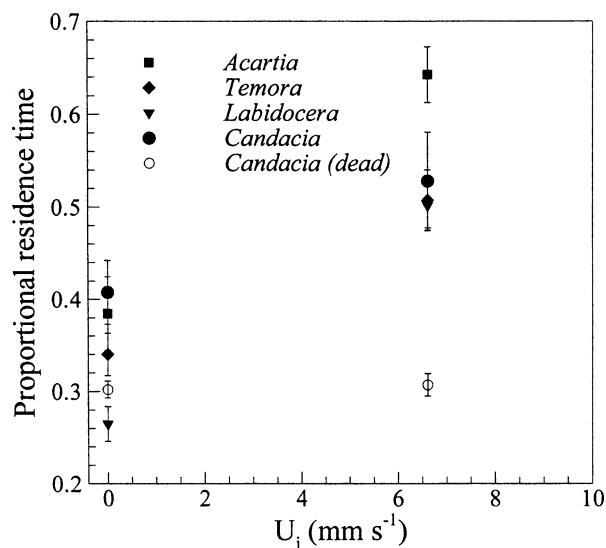
Fig. 5. Residence time in layer as proportion of total time in the field of view for the velocity gradient layer treatment (U_j = 6.7 mm s⁻¹). Control experiment is at U_j = 0 mm s⁻¹.
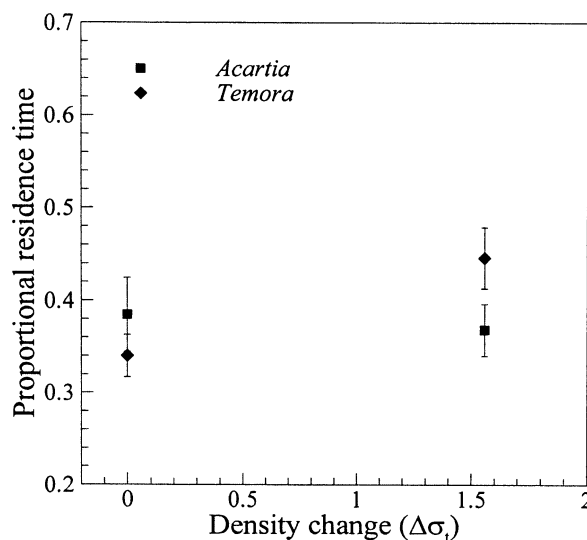

Fig. 6. Residence time in layer as proportion of total time in the field of view for the density-gradient layer treatment ($\Delta\sigma_t$ = 1.8). Control experiments correspond to constant salinity ($\Delta\sigma_t$ = 0).

trol experiments for all species range from 0.33 to 0.40, close to the values expected because the layer comprised one third to two fifths of the observation section. Proportional residence times of recently dead, undamaged *C. ethiopica* were not affected by the presence of a velocity gradient (Fig. 5, degrees of freedom = 39, F = 0.08, p = 0.779). Therefore, increases in residence time for the velocity gradient layer treatment are attributed to changes in the behavior of live organisms.

T. longicornis and *A. tonsa* remained in the velocity gradient layer by increasing swimming speed and turning more frequently (Tables 1 and 2; Fig. 7a,b). Swimming paths of both species in the control experiments (Fig. 7e,f) were much straighter. Average relative swimming speed for all four species increased when animals contacted the velocity gradient (Table 1; degrees of freedom = 93, F = 7.03, p = 0.009, *A. tonsa*; degrees of freedom = 86, F = 16.74, p < 0.001, *T. longicornis*; degrees of freedom = 87, F = 62.41, p < 0.001, *C. ethiopica*; degrees of freedom = 51, F = 13.02, p < 0.001, *L. madurae*) but were largely unaffected by the density gradient. Precontact swimming speeds for all copepods were comparable with control average swimming speed but not identical, possibly due to variation in the sex ratio between groups of animals in treatments versus controls (males often swim faster than females). However, note that statistical comparisons were conducted only between swimming speeds pre- and postcontact with the layer region. This analysis assures that variation among populations in different experiments does not bias the detection of responses to the density or velocity treatments. Control experiments for all species did not reveal any significant change between precontact and postcontact factors (Table 1).

Differences in the average turning rate significantly increased in the presence of the velocity gradient layer for both *A. tonsa* and *T. longicornis* over control (Table 2; degrees of freedom = 79, F = 18.83, p < 0.001, *A. tonsa*; degrees of freedom = 78, F = 4.06, p = 0.047, *T. longicornis*).

Significant differences in turn rate in layer and out of layer also were observed for both species (Table 2; degrees of freedom = 64, F = 5.92, p = 0.018, *A. tonsa*; degrees of freedom = 55, F = 4.17, p = 0.046, *T. longicornis*). *C. ethiopica* also exhibited a significant increase in turn rate between the velocity gradient and control experiments (degrees of freedom = 87, F = 12.13, p < 0.001). The increased turn rate for *L. madurae* in the velocity gradient treatment was not significant, possibly due to the low number of viable control paths for this analysis (Table 2; degrees of freedom = 50, F = 1.39, p = 0.24).

Table 1. Comparison of swimming speed for all species precontact and postcontact with the model thin layer region. An asterisk (*) denotes significant differences (p < 0.05) between precontact and postcontact values by single-factor ANOVA. Also tabulated is the coefficient of variance (COV) of swimming speed, for which only *T. longicornis* shows a significant difference in the layer.

Species Treatment	n	Precontact speed (mm s⁻¹) (SE)	COV	Postcontact speed (mm s⁻¹) (SE)	COV
Acartia tonsa					
Control	47	2.23 (0.17)	0.44	2.15 (0.15)	0.42
Velocity	47	3.08 (0.17)	0.35	3.68* (0.19)	0.39
Density	48	1.82 (0.07)	0.24	1.71 (0.06)	0.27
Temora longicornis					
Control	41	4.50 (0.41)	0.78	4.76 (0.47)	0.88
Velocity	46	5.40 (0.41)	0.87	6.84* (0.51)	1.83*
Density	48	5.37 (0.24)	1.32	5.36 (0.19)	1.60
Candacia ethiopica					
Control	47	3.52 (0.25)	0.81	3.61 (0.32)	0.82
Velocity	41	4.06 (0.26)	0.87	7.33* (0.47)	1.22
Labidocera madurae					
Control	15	4.89 (0.57)	1.10	4.80 (0.54)	0.96
Velocity	37	5.44 (0.36)	0.89	7.50* (0.41)	0.84

Table 2. Comparison of turn-event frequency for all species in layer and out of layer. A turn event is defined as a change of direction exceeding 15 degrees. An asterisk (*) denotes significant difference between in-layer and out-of-layer values ($p < 0.05$) by single-factor ANOVA.

Species Treatment	n	Turn rate (turns individual^{-1} s^{-1}) (SE)	Rate out of layer (turns individual^{-1} s^{-1}) (SE)	Rate in layer (turns individual^{-1} s^{-1}) (SE)
Acartia tonsa				
Control	40	0.06 (0.01)	—	—
Velocity	40	0.14 (0.02)	0.09 (0.02)	0.24* (0.05)
Density	40	0.07 (0.03)	0.06 (0.02)	0.08 (0.03)
Temora longicornis				
Control	40	0.11 (0.02)	—	—
Velocity	40	0.19 (0.03)	0.10 (0.02)	0.24* (0.06)
Density	40	0.14 (0.02)	0.13 (0.04)	0.14 (0.03)
Candacia ethiopica				
Control	40	0.09 (0.01)	—	—
Velocity	40	0.24 (0.04)	0.17 (0.04)	0.26 (0.08)
Labidocera madurae				
Control	15	0.17 (0.05)	—	—
Velocity	37	0.23 (0.03)	0.15 (0.04)	0.25 (0.06)

T. longicornis swimming in the presence of velocity gradients showed increased variability in speed in addition to an increase in average swimming speed. This increased variability is evident in comparisons of the coefficient of variation (COV) between precontact and postcontact paths of actively responding copepods. Other species showed no significant changes in the COV between precontact and postcontact. Only *C. ethiopica* showed an increase, but it was not statistically significant. *A. tonsa* (Table 1) did not show increased variability in swimming speed, likely due to a hop–sink swimming motion dominating statistical calculations.

All swimming speed measurements in the trials were within observed cruise-speed ranges for *T. longicornis* (2–12 mm s^{-1}) and *A. tonsa* (1–6 mm s^{-1}) and well below escape response speeds, which are greater than approximately 20 mm s^{-1} (Mauchline 1998). Observations of escape events for all species were rare, with less than five escape events occurring over sample sets of approximately 50 paths and were not included in the analysis.

Individual time records of *T. longicornis* in the control and velocity gradient treatments are plotted in Fig. 8 and illustrate the changes in speed of animals contacting the layer (Table 1). These records are selected because both animals enter the layer region at approximately 12 seconds (noted in figure). The treatment record revealed an increase for both mean swimming speed and variability in swimming speed within the layer compared with the control. The solid and dash–dot lines indicate the path average swimming speed with precontact and postcontact averages separated for the velocity treatment. Similar observations were made for *A. tonsa*.

Swimming speed for *A. tonsa* and *T. longicornis* increased after contact with the velocity layer (Figs. 9 and 10, respectively). The data points were partitioned into precontact and postcontact with the layer because some individuals that exit the layer region remain in an excited state associated with increased swimming speed. For both species, a strain rate of 0.025 s^{-1} appeared to be a reasonable estimate of the behavioral threshold value because the mean swimming speed appears to increase beyond this value (Figs. 9 and 10).

A better estimate of the actual behavioral strain rate threshold comes from analysis of individual swimming paths. A range of response thresholds were established for both *A. tonsa* and *T. longicornis* for the velocity gradient layer by comparing the behavior above and below an arbitrary threshold value (Fig. 11). This is accomplished by comparing the difference in the mean swimming speed, $\Delta\mu$, for data above and below a threshold value. The corresponding difference in the standard deviation, $\Delta\sigma$, was also calculated. The behavioral threshold was indicated by an abrupt change in $\Delta\mu$ and $\Delta\sigma$. For *A. tonsa,* $\Delta\mu$ increased with increasing threshold value because of their hop–sink swimming pattern. Swimming speed for this organism was dominated by low-velocity sinking periods, which were most frequent when organisms were not responding to the velocity gradient layer. Thus, $\Delta\mu$ increased at the behavioral threshold for shear strain rate (0.035–0.06 s^{-1}), above which the frequency of hopping bouts increased (Fig. 11a). Conversely, the cruise swimmer, *T. longicornis,* had an appreciable swimming speed prior to contacting the layer that increased after contact. Thus, $\Delta\mu$ declined past the behavioral threshold for shear strain rate (Fig, 11c, 0.015–0.03 s^{-1}) as swimming speeds on both sides of the threshold are dominated by rapid swimming speeds. The strain rate varied rapidly over a millimeter or so near the edge of the layer (Fig. 3); therefore, accounting for body length and mechanosensory array location in relation to the spatial gradient of shear strain rate, the range for behavioral response for *T. longicornis* was more likely between 0.03 and 0.06 s^{-1}. The range estimated for the smaller *A. tonsa* was not significantly affected by these considerations.
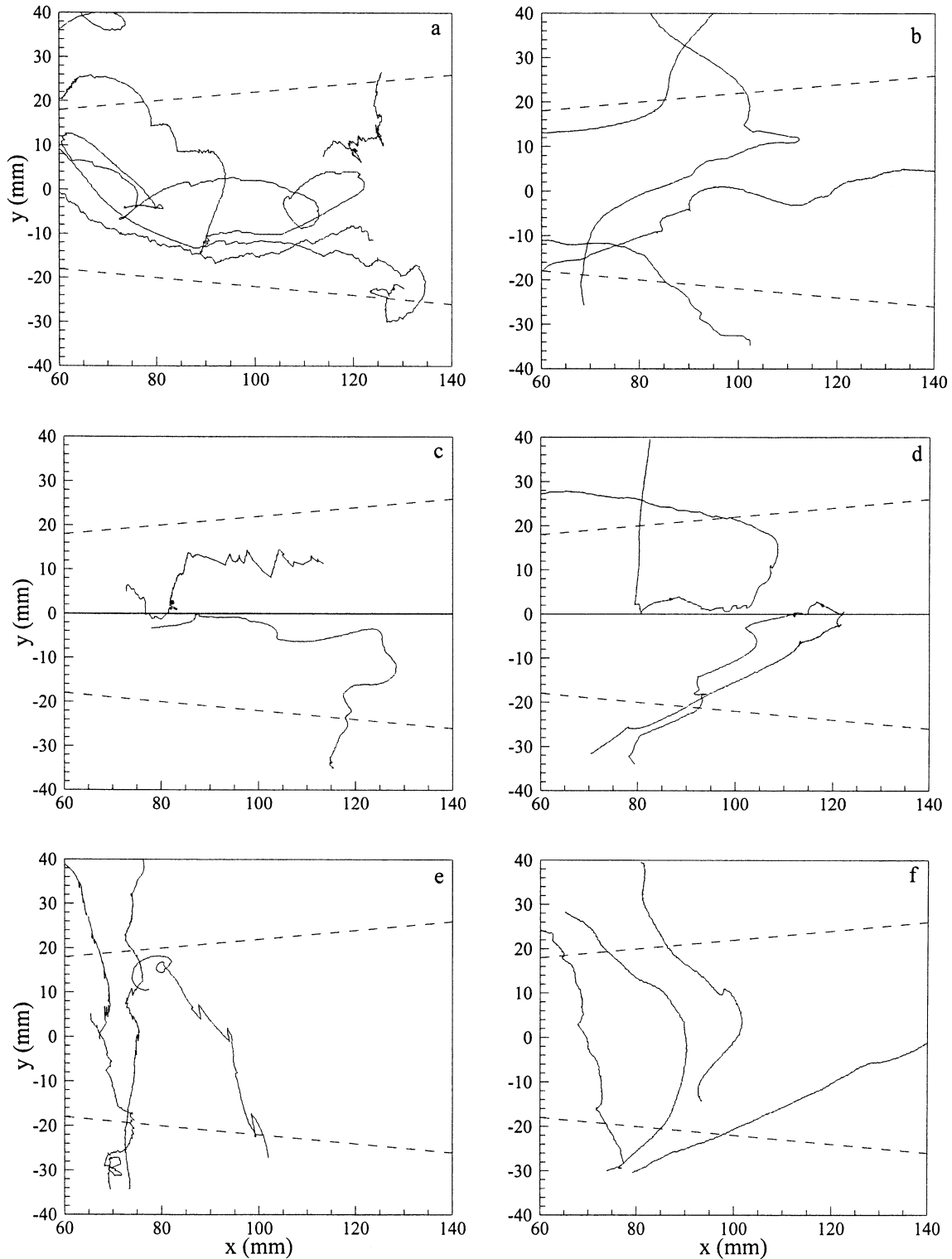
Fig. 7. Sample paths for *A. tonsa* (a, c, e) and *T. longicornis* (b, d, f) for the velocity gradient layer (a, b), the density-gradient layer (c, d), and control (e, f) treatments. The dashed lines indicate the edge of the layer corresponding to δ_s.

Although *T. longicornis* significantly increased residence time (Fig. 6) in response to the density-gradient layer (degrees of freedom = 99, $F = 6.86$, $p = 0.012$), swimming speed and turn frequency were not significantly different for both species tested under this condition (Tables 1 and 2). No statistical difference in swimming speed or turn frequency was observed in precontact versus postcontact or precontact and total versus control tests for both *T. longicornis* and *A.*
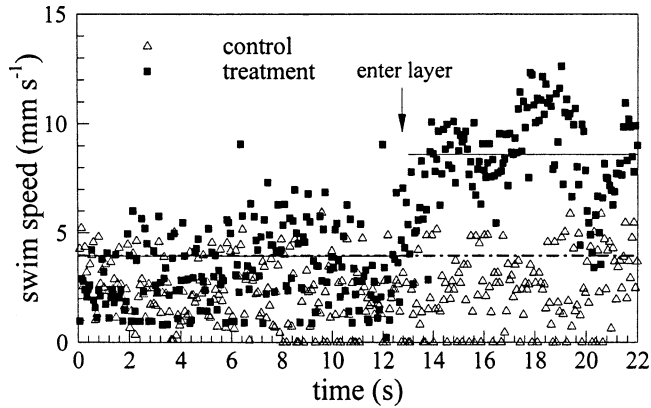
Fig. 8. Time record of swimming speed for two sample *T. longicornis* paths for the velocity gradient layer treatment. The solid line indicates the average value for the treatment path (in and out of layer indicated separately) and the dashed line indicates the average value for the control experiment.

tonsa. Sample paths from these experiments are shown in Fig. 7c,d. Both species were often observed to encounter the density gradient, turn, and swim along the layer or in the opposite direction in a manner similar to the copepod en-

countering a free surface or a fixed barrier. Direct observation of 40 paths from treatment and control experiments revealed significant differences in the number of copepods that crossed or did not cross the locale of the density gradient (Table 3).

Behavioral variability among individuals often prevents meaningful conclusions regarding the significance of a particular treatment because individuals respond in their own fashion (Figs. 7, 9–11). In this study, individual swimming paths were presented for demonstration purposes, and ensemble averages of animals prior to and subsequent to contact with the layer were used to show aggregate behavioral changes in the population. For example, ensemble-averaged swimming speed for *T. longicornis* in this study increased by 1.4 mm s^{-1}, a result of 34 individuals (out of 46) increasing swimming speed after contact with the velocity layer. All responsive individuals increased swimming speed by 1–2 mm s^{-1}.

Discussion

Copepods are known to aggregate at discontinuities in the water column (Cowles et al. 1998; Holliday et al. 1998; Dekshenieks et al. 2001) and maintain position in regions of high
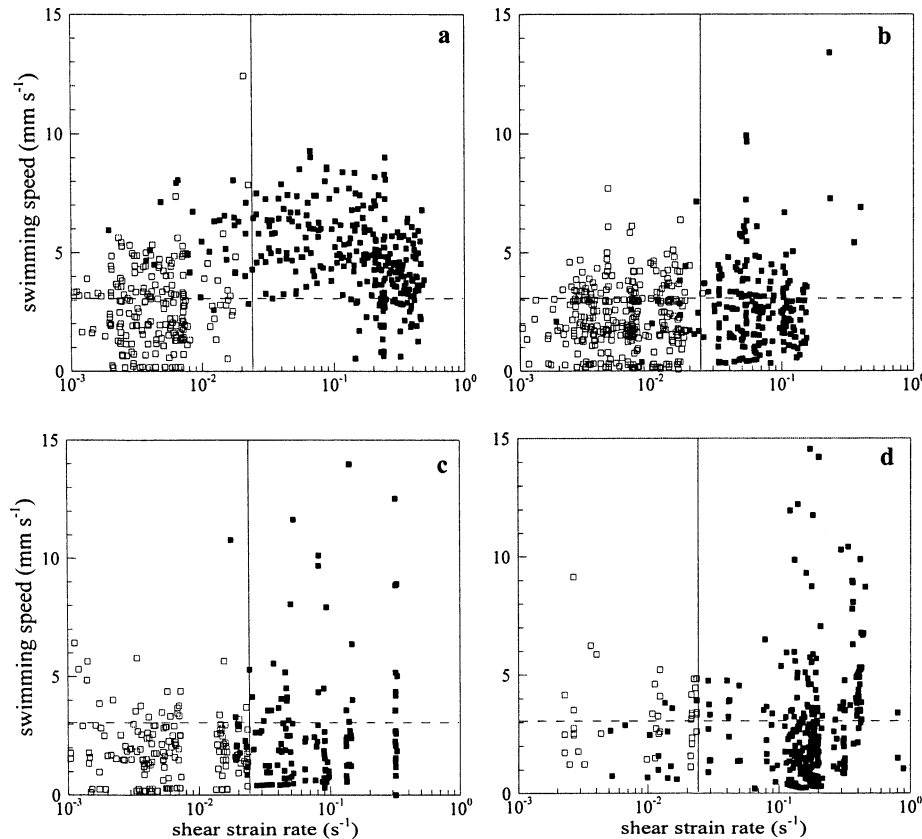

Fig. 9. Swimming speeds for *A. tonsa* plotted against shear strain rate for the velocity gradient layer treatment for four individuals (a–d). Open squares, precontact; solid squares, postcontact with the layer. The solid vertical line shows the shear strain rate level (0.025 s^{-1}) at the edge of the layer. The dashed line shows the average swimming speed for all trials. All shear strain rate data were based on the centroid location of the animals.
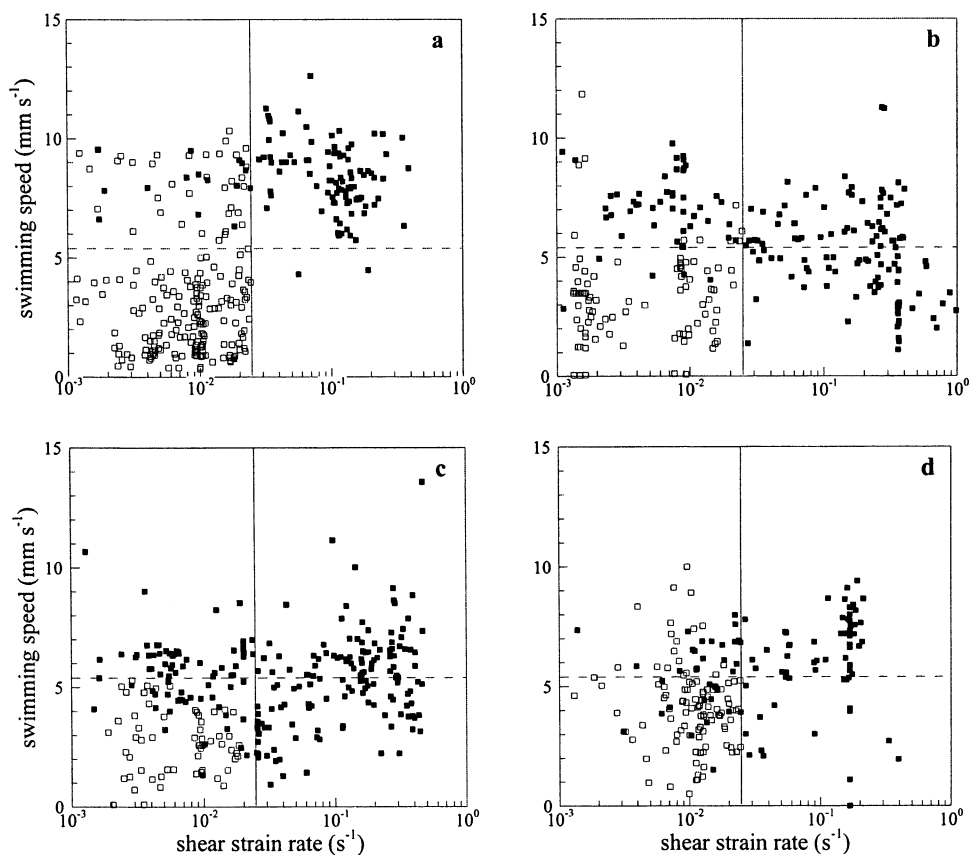
Fig. 10. Swimming speeds for *T. longicornis* plotted against shear strain rate for the velocity gradient layer treatment for four individuals (a–d). Open squares, precontact; solid squares, postcontact with the layer. The solid vertical line shows the shear strain rate level (0.025 s^{-1}) at the edge of the layer. The dashed line shows the average swimming speed for all trials. All shear strain rate data were based on the centroid location of the animals.

food concentration (Tiselius 1992). In order to alter behavior and maintain position in these regions, copepods must be able to sense and react to the properties associated with these patches. Cowles et al. (1998) and Dekshenieks et al. (2001) report the important characteristics of oceanic structure as sharp gradients of velocity, fluid density, biological activity, and chemical concentration. Gallager et al. (2004) observed in situ copepod aggregations associated with physical structure in the ocean and suggested behavioral mechanisms for these occurrences. In this study, we have addressed the ability of four copepod species, *A. tonsa, T. longicornis, C. ethiopica,* and *L. madurae,* to react to a velocity gradient (or shear) layer and the response of two species, *A. tonsa* and *T. longicornis,* to a density-gradient layer. Ranges of stain rate and the density change in the experiments span those reported from field studies and are likely to be encountered in nature by the species tested.

Temporal and spatial scales in the field are often hard to match in the laboratory. In this study, the gradient layer was approximately 4 cm thick, with shear strain rates ranging between 0 and 0.35 s^{-1}, and a density jump near 1.8 σ_t units. The thickness of the layer is below reported minimum thicknesses (10 cm) from the field; however, field estimates are still limited by resolution (Cowles 2004). Thinner layers,

higher shear strain rates, and steeper density gradients than have been reported to date may be present in the ocean. For the current behavioral response study, the important length scale is that of an individual copepod (i.e., 1 mm). The laboratory layer was very large (roughly 4 cm) compared with the copepod, so individuals cannot sense the upper and lower edges of the layer simultaneously. Therefore, from the perspective of the copepod, the fluid deformation (quantified by the shear strain rate) is similar in our model layer to that in an oceanic thin layer. This study observed rapid responses of individuals, that at the population level could lead to observed aggregations and suggests that measurements in the open ocean may need to be performed at a higher resolution in order to characterize features relevant to actively behaving zooplankton.

The species examined in this study exhibited behaviors congruent with area-restricted search behavior (Buskey 1984; Turchin 1991; Mauchline 1998). Increased swimming speed, variation in speed, and turn frequency within the layer suggest that these animals were excited by the presence of the velocity gradient in a positive fashion and were attempting to remain in the layer. Velocity gradients may act as an initial cue to the presence of a new water body, thus instigating area-restricted search. Copepods eventually cease lo-
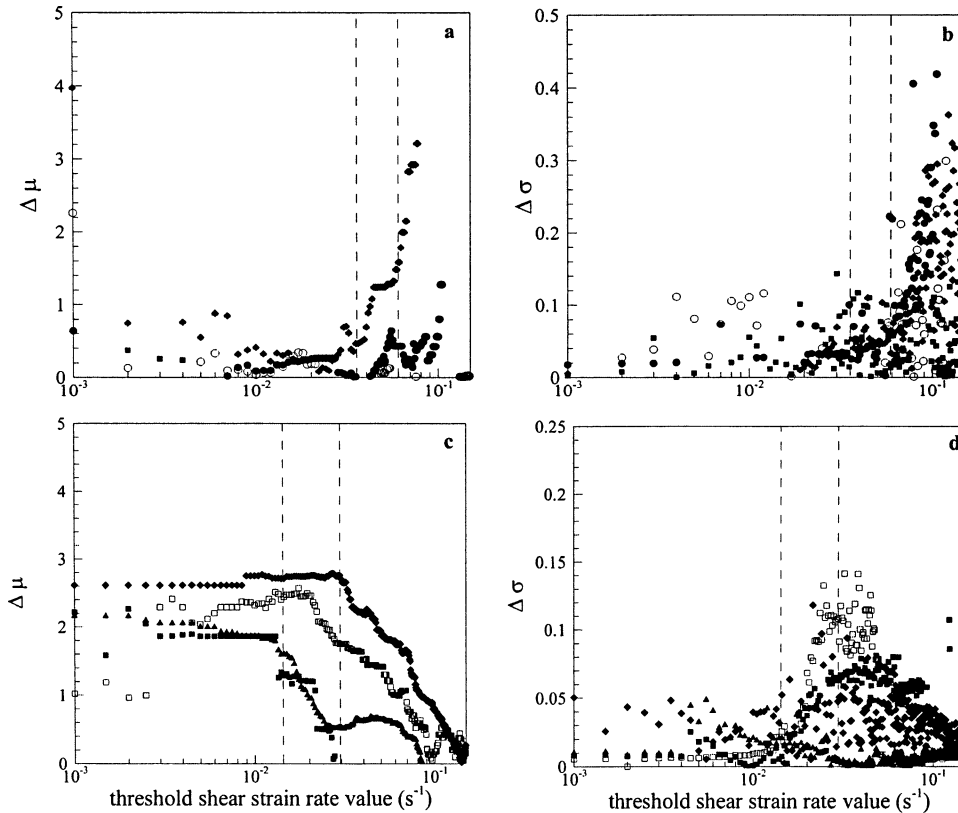
Fig. 11. Defining the threshold shear strain rate values for *A. tonsa* (a, b) and *T. longicornis* (c, d) in the velocity gradient layer. Data from five sample paths are shown in each figure. $\Delta\mu$ (a, c) is defined as the difference between the mean swimming speed value calculated for data above and below a threshold shear strain rate value. $\Delta\sigma$ (b, d) is calculated as the difference between the standard deviation calculated for swimming speed data above and below a threshold shear strain rate value. An abrupt change in the difference indicates a behavior transition and hence suggests an individual threshold for behavioral response.

cal searching and continue random-directed movement if no further cue is present (i.e., food presence or chemical component). If food or chemical stimuli are associated with changes in flow velocity, then velocity gradients would act as a cue to initiate aggregative or swarming behavior in these regions, thus increasing search success by limiting active searching areas. The presence of a resource such as food would negate the area-restricted search response and cue

Table 3. Response of *A. tonsa* and *T. longicornis* to density gradient ($\Delta\sigma_t = 1.8$) compared with control ($\Delta\sigma_t = 0.0$). Two-tailed *p*-values are from Fisher's exact test.

Species Treatment	*n*	Crossed gradient locale	Did not cross gradient locale	*p*
Acartia tonsa				
Control	40	26	14	—
Density	40	9	31	<0.001
Temora longicornis				
Control	40	27	13	—
Density	40	15	25	0.013

feeding behavior resulting in lower average swimming speed, as observed by Tiselius (1992).

Responses to the density-gradient layer were strikingly different than responses to velocity gradients. *A. tonsa* did not increase proportional residence time in the density-gradient layer experiments (0.37 vs. 0.39 for the control). Even though *T. longicornis* did significantly increase proportional residence time in the density-gradient layer (0.45) compared with that for the control (0.34), other behavioral markers were not significantly different. Evaluation of the paths showed that individuals of both species made contact with the density gradient and then either swam along the gradient layer or turned and swam away. This was a significant behavioral change created by the density gradient and similar to a copepod swimming near the water surface or bottom of the tank. Hence, sharp density gradients may act as barriers to vertical migration for copepods, thus resulting in aggregations at these boundaries due to a physical or a behavioral barrier. These observations are consistent with hypotheses and arguments posed by Harder (1968) and Gallager et al. (2004).

Our results suggest that gradients of two important physical properties of oceanic water bodies, current velocity and

fluid density, appear to have differing effects on individual copepods. Velocity gradients seem to act as a positive cue for area-restricted search behavior, which can lead to aggregation over larger time scales (Hamner 1988; Turchin 1991; Tiselius 1992; Leising and Franks 2000). Density gradients appear to be physical or behavioral barriers to vertical migration, which may also lead to aggregation (Tiselius 1992; Lougee et al. 2002; Bochdanksy and Bollens 2004; Clay et al. 2004). The extent that these gradients affect populations and communities is still not understood, but results here suggest that, from the perspective of a copepod, the ocean is a structured and patterned habitat at scales much smaller than historically accepted (Hutchinson 1961; Yamazaki et al. 2002; Cowles 2004). The influence of individual behavior on pattern in pelagic habitats warrants further investigation at the fine-to-intermediate scales (millimeter to meter), and emphasis on better resolution in field measurements, combined with continued laboratory investigations, is imperative to developing our understanding of zooplankton behavior and ecology at appropriate scales.

References

ALLDREDGE, A. L., AND OTHERS. 2002. Occurrence and mechanisms of formation of a dramatic thin layer of marine snow in a shallow Pacific fjord. Mar. Ecol. Prog. Ser. **233:** 1–12.

BICKLEY, W. G. 1937. The plane jet. Philosophical Magazine Series 7 **23:** 727–731.

BOCHDANSKY, A. B. AND S. M. BOLLENS. 2004. Relevant scales in zooplankton ecology: Distribution, feeding, and reproduction of the copepod *Acartia hudsonica* in response to thin layers of the diatom *Skeletonema costatum.* Limnol. Oceanogr. **49:** 625–636.

BUSKEY, E. J. 1984. Swimming pattern as an indicator of the roles of copepod sensory systems in the recognition of food. Mar. Biol. **79:** 165–175.

CLAY, T. W., S. M. BOLLENS, A. B. BOCHDANSKY, AND T. R. IGNOFFO. 2004. The effects of thin layers on the vertical distribution of larval Pacific herring, *Clupea pallasi.* J. Exp. Mar. Biol. Ecol. **305:** 171–189.

COWLES, T. J. 2004. Planktonic layers: Physical and biological interactions on the small scale, p. 31–49. *In* L. Seuront and P. G. Strutton [eds.], Handbook of scaling methods in aquatic ecology: Measurements, analysis, simulation. CRC Press.

———, R. A. DESIDERIO, AND M.-E. CARR. 1998. Small-scale planktonic structure: Persistence and trophic consequences. Oceanography **11:** 4–9.

DARO, M. H. 1988. Migratory and grazing behavior of copepods and vertical-distribution of phytoplankton. Bull. Mar. Sci. **43:** 710–729.

DASI, L. P. 2004. The small-scale structure of passive scalar mixing in turbulent boundary layers. Ph.D. thesis, Georgia Institute of Technology.

DEKSHENIEKS, M. M., P. L. DONAGHAY, J. M. SULLIVAN, J. E. B. RINES, T. R. OSBORN, AND M. S. TWARDOWSKI. 2001. Temporal and spatial occurrence of thin phytoplankton layers in relation to physical processes. Mar. Ecol. Prog. Ser. **223:** 61–71.

FIELDS, D. M., D. S. SHAEFFER, AND M. J. WEISSBURG. 2002. Mechanical and neural responses from the mechanosensory hairs on the antennule of *Gaussia princeps.* Mar. Ecol. Prog. Ser. **227:** 173–186.

———, AND J. YEN. 1997a. The escape behavior of marine copepods in response to a quantifiable fluid mechanical disturbance. J. Plankton Res. **19:** 1289–1304.

———, AND ———. 1997b. Implications of the feeding current structure of *Euchaeta rimana,* a carnivorous pelagic copepod, on the spatial orientation of their prey. J. Plankton Res. **19:** 79–95.

FRANKS, P. J. S. 1995. Thin-layers of phytoplankton—a model of formation by near-inertial wave shear. Deep-Sea Res. I **42:** 75–91.

GALLAGER, S. M., H. YAMAZAKI, AND C. S. DAVIS. 2004. Contribution of fine-scale vertical structure and swimming behavior to formation of plankton layers on Georges Bank. Mar. Ecol. Prog. Ser. **267:** 27–43.

HAMNER, W. M. 1988. Behavior of plankton and patch formation in pelagic ecosystems. Bull. Mar. Sci. **43:** 752–757.

HARDER, W. 1968. Reactions of plankton organisms to water stratification. Limnol. Oceanogr. **13:** 156–168.

HOLLIDAY, D. V., P. L. DONAGHAY, C. F. GREENLAW, D. E. McGEHEE, M. M. McMANUS, J. M. SULLIVAN, AND J. L. MIKISS. 2003. Advances in defining fine- and micro-scale pattern in marine plankton. Aquatic Living Resources **16:** 131–136.

———, R. E. PIEPER, C. F. GREENLAW, AND J. K. DAWSON. 1998. Acoustical sensing of small-scale vertical structures in zooplankton assemblages. Oceanography **11:** 18–23.

HUSSEIN, H. J. 1994. Evidence of local axisymmetry in the small scales of a turbulent planar jet. Physics of Fluids **6:** 2058–2070.

HUTCHINSON, G. E. 1961. The paradox of the plankton. Am. Nat. **95:** 137–145.

KIØRBOE, T., E. SAIZ, AND A. VISSER. 1999. Hydrodynamic signal perception in the copepod *Acartia tonsa.* Mar. Ecol. Prog. Ser. **179:** 97–111.

LEISING, A. W. 2001. Copepod foraging in patchy habitats and thin layers using a 2-D individual-based model. Mar. Ecol. Prog. Ser. **216:** 167–179.

———, AND P. J. S. FRANKS. 2000. Copepod vertical distribution within a spatially variable food source: A simple foraging-strategy model. J. Plankton Res. **22:** 999–1024.

LOUGEE, L. A., S. M. BOLLENS, AND S. R. AVENT. 2002. The effects of haloclines on the vertical distribution and migration of zooplankton. J. Exp. Mar. Biol. Ecol. **278:** 111–134.

MAUCHLINE, J. 1998. The biology of calanoid copepods. Elsevier Academic Press.

MULLIN, M. M., AND E. R. BROOKS. 1976. Some consequences of distributional heterogeneity of phytoplankton and zooplankton. Limnol. Oceanogr. **21:** 784–796.

POULET, S. A., AND P. MARSOT. 1978. Chemosensory grazing by marine calanoid copepods (Arthropoda Crustacea). Science **200:** 1403–1405.

———, AND G. OUELLET. 1982. The role of amino acids in the chemosensory swarming and feeding of marine copepods. J. Plankton Res. **4:** 341–361.

RAFFEL, M., C. WILLERT, AND J. KOMPENHANS. 1998. Particle image velocimetry: a practical guide. Springer.

SAIZ, E., P. TISELIUS, P. R. JONSSON, P. VERITY, AND G.-A. PAFFENHOFER. 1993. Experimental records of the effects of food patchiness and predation on egg production of *Acartia tonsa.* Limnol. Oceanogr. **38:** 280–289.

SATO, H., AND F. SAKAO. 1964. An experimental investigation of the instability of a two-dimensional jet at low Reynolds numbers. J. Fluid Mech. **20:** 337–352.

STRICKLER, J. R. 1977. Observation of swimming performances of planktonic copepods. Limnol. Oceanogr. **22:** 165–169.

———. 1998. Observing free-swimming copepods mating. Phil. Trans. R. Soc. B **353:** 671–680.

TISELIUS, P. 1992. Behavior of *Acartia tonsa* in patchy food environments. Limnol. Oceanogr. **37:** 1640–1651.

———, G. NIELSEN, AND T. G. NIELSEN. 1994. Microscale patchiness of plankton within a sharp pycnocline. J. Plankton Res. **16:** 543–554.

TITELMAN, J. 2001. Swimming and escape behavior of copepod nauplii: Implications for predator–prey interactions among copepods. Mar. Ecol. Prog. Ser. **213:** 203–213.

———, AND T. KIØRBOE. 2003*a.* Motility of copepod nauplii and implications for food encounter. Mar. Ecol. Prog. Ser. **247:** 123–135.

———, AND ———. 2003*b.* Predator avoidance by nauplii. Mar. Ecol. Prog. Ser. **247:** 137–149.

TURCHIN, P. 1991. Translating foraging movements in heterogeneous environments into spatial distribution of foragers. Ecology **72:** 1253–1266.

WEBSTER, D. R., S. RAHMAN, AND L. P. DASI. 2003. Laser-induced fluorescence measurements of a turbulent plume. J. Eng. Mech. **129:** 1130–1137.

YAMAZAKI, H., D. L. MACKAS, AND K. L. DENMAN. 2002. Coupling small-scale physical processes with biology, p. 51–112. *In* J. J. McCarthy and B. J. Rothschild [eds.], The sea, V. 12. John Wiley and Sons.

YEN, J., AND D. M. FIELDS. 1992. Escape responses of *Acartia hudsonica* (Copepoda) nauplii from the flow field of *Temora longicornis* (Copepoda). Arch. Hydrobiol. Beih. **36:** 123–134.

———, M. J. WEISSBURG, AND M. H. DOALL. 1998. The fluid physics of signal perception by mate-tracking copepods. Phil. Trans. R. B **353:** 787–804.